Single-molecule imaging and spectroscopy of the π-conjugated polymer MEH-PPV

Oleg Mirzov

Licentiate thesis

2006

Lund University

Contents

Abstract

This licentiate thesis is intended to give a short introduction into the field of single-molecule spectroscopy of π-conjugated polymers (Chapter 1) and to present a part of the work done by the author (in collaboration with other researchers) in this area. In this work single-molecule imaging and spectroscopy techniques, whose experimental implementation is described in Chapter 2, were used to study the π-conjugated polymer MEH-PPV. The spectroscopy technique was used to establish a "bridge" between single-molecule and "bulk" spectroscopy by investigating a range of samples with different concentrations of MEH-PPV: from films to single chains (Chapter 3). Single-molecule imaging was employed to study fluorescence intensity distributions of single MEH-PPV chains, thereby addressing the problem of a single-molecule quantum yield (Article I).

Chapter 1

Introduction

1.1 Single-molecule spectroscopy

Conventional optical spectroscopy studies a macroscopic sample with the purpose of obtaining information about sample structure and properties. The sample consists of molecules and, consequently, its spectral properties are determined by spectral properties of the molecules. Finally, spectral properties of the molecules are defined not only by their structure, but also by a local environment. Since no macroscopic sample is homogeneous on a microscopic level, this local environment differs from one molecule to the next. Therefore, any spectral property of a macroscopic sample, as observed with conventional optical spectroscopy, is a result of some sort of an averaging over the properties of the molecules comprising the sample. This phenomenon is called inhomogeneous broadening. Its main negative effect is the loss of spectral structure and the consequent loss of information about sample properties.

The most natural way to overcome this problem is to study only one molecule as a sample. However, this is an experimental challenge that could not be met until 1989, when the first paper on optical detection of single molecules was published by Moerner and Kador [1]. This work was followed shortly by a contribution from M. Orrit *et. al.* [2] who introduced single-molecule spectroscopy of dye molecules by means of fluorescence excitation in 1990.

One of the most spectacular effects observed with single-molecule spectroscopy is so-called fluorescence intermittency (or blinking effect) [3]. This phenomenon consists in interrupted fluorescence of a single molecule excited with a continuous light source (Fig. 1.1). The reason for fluorescence interruption is quantum jumps of the molecule from the first singlet excited state to the first triplet excited state, which is lower in energy. Radiative transition from the triplet state is forbidden, so the molecule can stay in this state for a long time (up to milliseconds or even

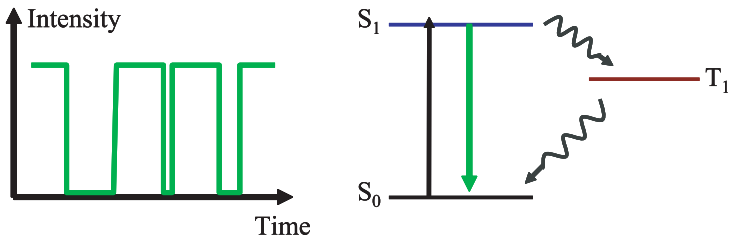

Figure 1.1: Blinking effect in dye molecules.

more depending on the system) without absorption and emission of photons. Then the molecule relaxes back into the ground state non-radiatively, and the process repeats itself.

Another well-known intrinsically single-molecule effect discovered with the new technique was so-called spectral diffusion [4]. This is a phenomenon of absorption frequency change in a single molecule, resulting from a change in its photophysical parameters or a change in local environment. Later it was shown that fluorescence spectrum of a single dye molecule fluctuates as well [5].

1.2 Π-conjugated polymers

Π-conjugated polymers can be defined as organic polymers with π and π^* molecular orbitals delocalized over the whole polymer chain. In the language of chemical structural formulae, these orbitals are represented as an alternation of single and double carbon bonds along the chain (Fig. 1.2). Another characteristic feature of

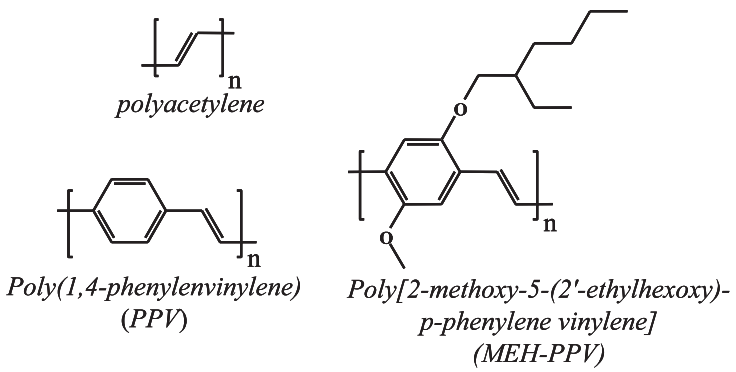

Figure 1.2: Structural formulae of some π-conjugated polymers.

these formulae is that it is possible to swap the positions of the single and double

bonds and end up with a structure that still satisfies the chemical-bonding requirements for carbon.

A lot of research effort has been concentrated on these polymers since the discovery of high conductance in doped polyacetylene [6, 7] by A.J. Heeger, A.G. MacDiarmid, H. Shirakawa, *et. al.* in 1977. In the year 2000 these researchers have been awarded a Nobel Prize in chemistry for this discovery [8]. The reason for such strong interest in π-conjugated polymers is rooted in a unique combination of properties these materials possess.

To get an insight into these properties, it is helpful to consider how π and π^* molecular orbitals are formed from the point of view of the linear combination of atomic orbitals technique (Fig. 1.3). Two of the three 2p orbitals on

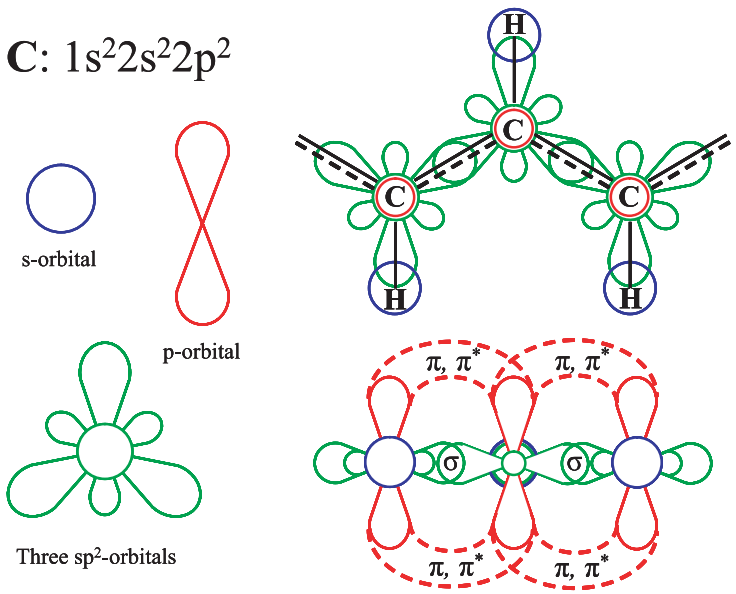

Figure 1.3: A scheme of molecular orbital formation in π-conjugated polymers.

each carbon atom combine with the 2s orbital to form three sp^2 "hybrid" orbitals. These orbitals lie in a plane, directed at 120° to one another, and form three σ molecular orbitals with neighbouring atoms, including one with hydrogen. The third p-orbital on the carbon atom points perpendicular to the sp^2-orbital plane. It overlaps with the other non-hybrid p-orbitals on neighbouring carbon atoms to form a pair of molecular orbitals: π (bonding) and π^* (anti-bonding). Since electrons can have two different spin states, the lower-energy bonding π-orbital gets occupied, and the higher energy anti-bonding π^*orbital is left unoccupied. The resulting electronic structure of π-conjugated polymers is similar to that of semiconductors (Fig. 1.4). Indeed, the highest occupied molecular orbital (HOMO)

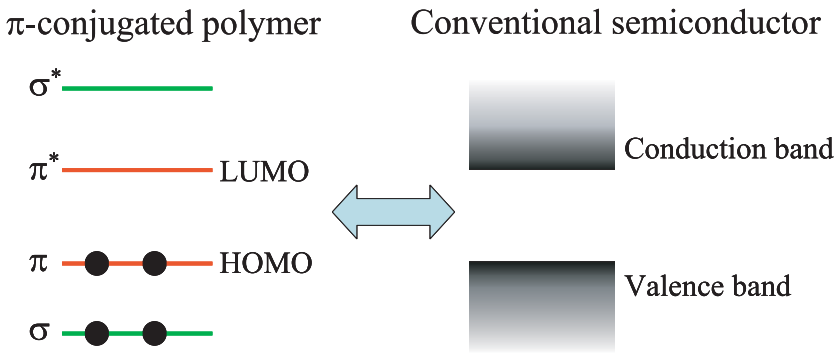

Figure 1.4: The analogy between π-conjugated polymers and semiconductors.

is analogous to the valence band edge in semiconductors, the lowest unoccupied molecular orbital (LUMO) — to the conduction band edge, and the gap between them is analogous to the semiconductor band gap. Most conjugated polymers have semiconductor band gaps of 1.5-3 eV, which means that they are suitable for optoelectronic devices that emit visible light. It is the combination of fluorescence and semiconducting properties together with processability of plastics that makes these materials so attractive for applications.

However, the above picture holds only in the ideal case of perfectly straight polymer chains and absence of chemical defects. In reality such imperfections break the conjugation and "chop" the π-orbitals into "pieces" called spectroscopic units [9] (Fig. 1.5). The typical length of a spectroscopic unit is ~ 5 monomer

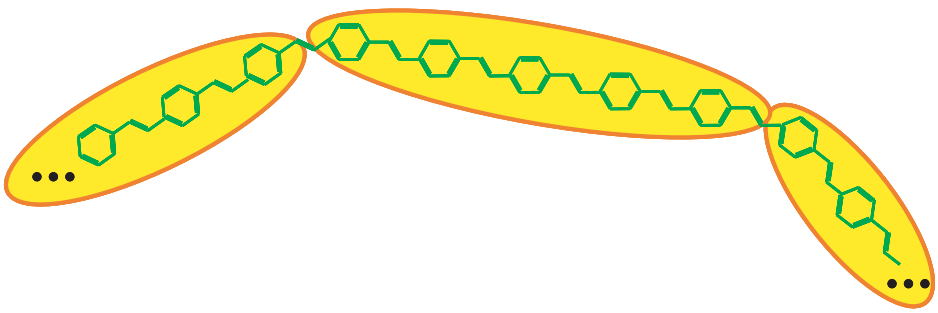

Figure 1.5: Spectroscopic units.

units for MEH-PPV [10]. Such a polymer chain is no longer a single semiconductor "crystal" but a series of chemically connected oligomers with semiconductor-like electronic structure. In was found to be more appropriate to describe electronic excited states in this system in terms of the exciton (correlated electron-hole

pair) picture rather than the true band gap (i.e., corresponding to separated, free electron and hole) picture of semiconductors [11, 12].

1.3 Single-molecule spectroscopy of π-conjugated polymers

We have seen that π-conjugated polymers are ensembles of spectroscopic units rather than single light-absorbing chromophores. Therefore, they may seem completely inappropriate objects for studying with single-molecule spectroscopy. Indeed, the ensembles of chromophores they consist of should make them indistinguishable from a bulk material. However, this was proven not to be the case with a discovery of fluorescence intensity fluctuations (blinking effect) in single chains of a multichromophoric conjugated polymer [13]. Apart from that, single π-conjugated polymer molecules were found to possess very individual fluorescence spectral properties, especially at low temperature [14, 15, 16, 17, 18]. Besides, fluorescence spectral diffusion was observed in single conjugated polymer chains recently [16], and the diffusion range reached as much as 1000 cm^{-1} [17, 18] (Fig. 1.6). Finally, an attempt to address the issue of photoluminescence

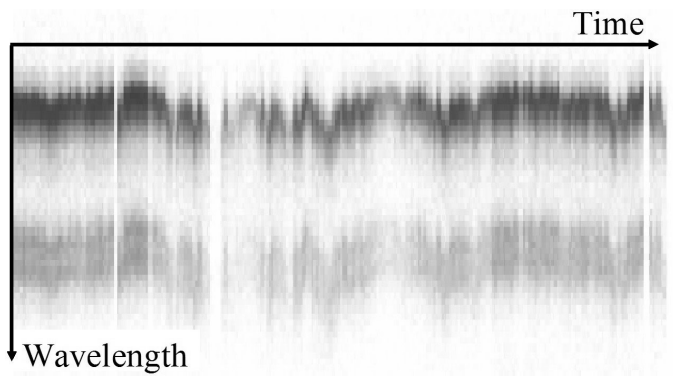

Figure 1.6: Fluorescence spectrum fluctuations in a single MEH-PPV molecule.

quantum yield in single π-conjugated polymer chains revealed that the quantum yield also differs a lot from one molecule to the next [19] (Article I).

One cannot expect to observe the abovementioned phenomena in an ensemble of independent non-interacting chromophores. There is no generally accepted explanation of all these phenomena at the moment. However, it can be considered as a well-established fact that there is an efficient excitation energy transfer between the spectroscopic units: all the excitons in a polymer chain get "funneled"

downhill in energy to a few (or even only one) spectroscopic unit referred to as exciton trap [20]. The exciton traps have local minima of excited state energy, so the exciton migration is a relaxation process. Hence, the polymer molecule acts as an ensemble of chromophores when absorbing photons, but only a few of the chromophores actually emit light (Fig. 1.7). This fact makes single-molecule spectroscopy a perfectly appropriate tool to study π-conjugated polymers.

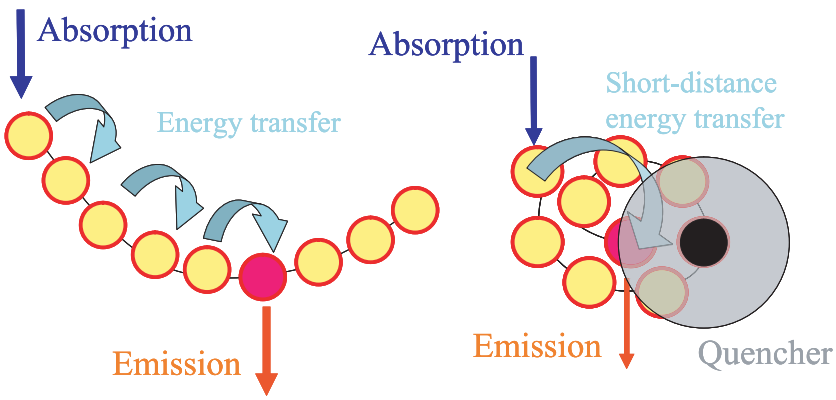

Figure 1.7: Excitation energy transfer to an exciton trap (left part) and partial fluorescence quenching for the case of a polymer chain with collapsed conformation (right part).

To explain the blinking effect, it was suggested that either the energy funnel reversibly switches to a long-lived dark state, or all (or part of) the excitons gets quenched by an external long-lived quencher [13, 20]. In the latter case the concept of energy funnels is not indispensable for explaining the effect: the quencher can quench all excitations regardless of their positions [21, 22] because the polymer chains often possess collapsed conformations [23] (Fig. 1.7, right part).

The observed fluorescence spectral diffusion does not have an established explanation yet. The suggested explanations include the presence of charges on and around the polymer chain [16] and dispersive interactions of the emitting chromophore with the environment, affected by conformational fluctuations [17].

Chapter 2

Experimental technique

2.1 Sample preparation

Since we are interested in studying spectroscopic properties of single molecules, the molecules should not only be separated from each other so that they do not interact in any way, but also the distance between them should be greater than the optical resolution of experimental setup. In this situation environmental conditions may be somewhat different for different molecules, thereby creating inhomogeneous broadening not inherent to the molecules as such. To minimize this effect, one may want to enclose the molecules into a relatively homogeneous chemically inert polymer host matrix. Alternatively, one can use a cap matrix rather than a host matrix, if only protecting the molecules against atmospheric oxygen is important. The typical sample structure used in this study is shown in Fig. 2.1. In this

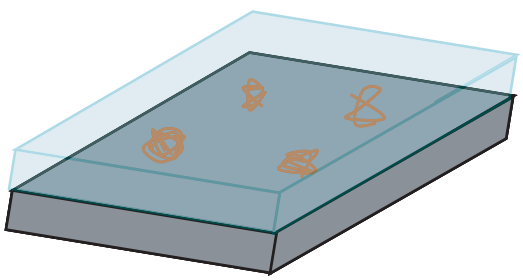

Figure 2.1: The sample structure.

work oxidized silicon wafers were used as substrates. Poly (methyl methacrylate) (PMMA) was used as a host matrix (Chapter 3), and poly (vinyl-alcohol) (PVA) — as a cap matrix (Article I).

MEH-PPV (Fig. 1.2) was chosen as a conjugated polymer to be studied. Two

polymer samples were investigated. One of them was purchased from Sigma-Aldrich and is known to have the number-average molecular weight M_N in the range 150 000–250 000 and polydispersity $P_M = 1.06$. Another one was manufactured by American Dye Source (ADS), Inc ($M_N = 105\,000$, $P_M \approx 7.8$). Only the Aldrich sample was used for the experiments in Chapter 3. See Article I, subsection 2.1 for more details about the polymer samples and the definitions of M_N and P_M.

To prepare the substrates for polymer deposition, a special cleaning routine was applied. First, the wafers were cleaned mechanically with a standard detergent for washing glassware. Then they were rinsed in toluene, dried, and rinsed with deionized water. After that the substrates were kept in a "piranha" mixture (1:2 H_2O_2:H_2SO_4) at $\approx 60\,^{\circ}C$ for ≈ 20 minutes to eat away any organic impurities. Then the wafers were rinsed with ultra-pure Milli-Q® water very thoroughly. To prevent subsequent precipitation of impurities from the air onto the substrates, they were left to be stored in Milli-Q® water. All of the above steps apart from the "piranha" treatment were performed in an ultra-sonic bath. Finally, just before depositing the polymer layers, the substrates were taken out of Milli-Q® water, rinsed once again, dried with a jet of nitrogen and kept under a UV-lamp for half an hour to photobleach the remaining fluorescent impurities.

To deposit the polymer layers, a standard spin-coating technique was employed. Spin-coating implies either putting a droplet of a solution onto the center of a rotating substrate, or first putting the solution onto the substrate and then spinning it up (Fig. 2.2). In this work the latter approach was used. The angular

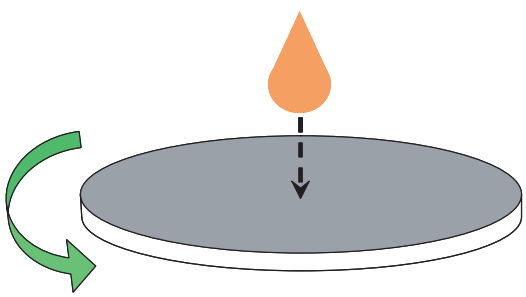

Figure 2.2: An illustration of the spin-coating technique.

velocity was 3000 rpm and toluene was used as a solvent. The solution concentration of MEH-PPV for single-molecule samples was $\sim 10^{-5}$ g/L. Apart from single-molecule samples, MEH-PPV films with varied thickness were studied in the experiments of Chapter 3. There the solution concentrations varied from 10^{-5} to 2 g/L. The latter solution concentration resulted in bulk polymer films rather than single-molecule samples.

2.2 Wide-field microscopy

One of the possible implementations of single-molecule spectroscopy is called wide-field fluorescence microscopy. The principle of the technique consists in using a fluorescence microscope to study the samples described above. Fluorescence microscope is a light microscope used to excite samples with a light and to observe the resulting photoluminescence coming from the samples. The scheme of the experimental setup is shown in Fig. 2.3. The 458 nm (Chapter 3) and 488

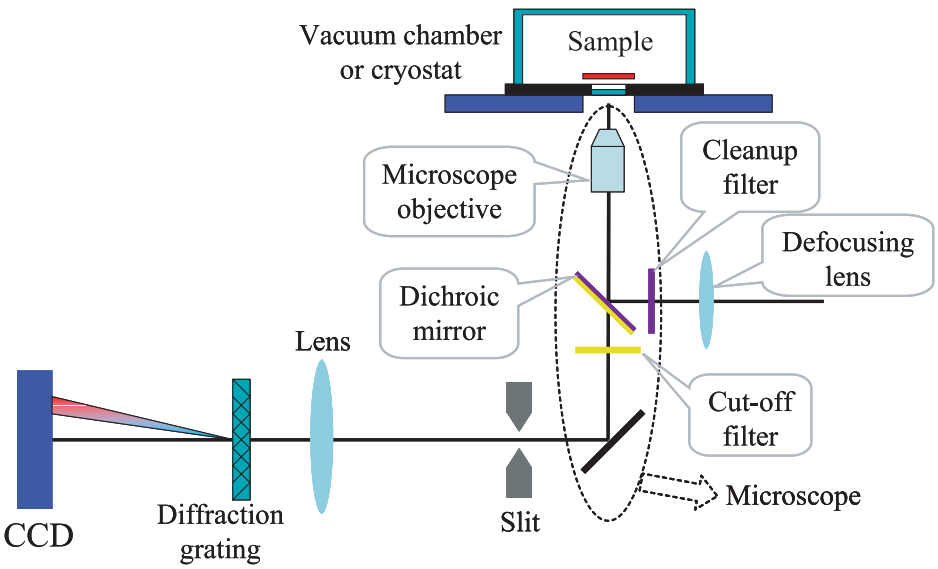

Figure 2.3: A scheme of the experimental setup.

nm (Article I) continuous Ar^+ laser lines were used for excitation. The excitation beam was steered into the microscope through a defocusing lens and run through a microscope objective (Olympus, LUCPlanFI, 40×, N.A. 0.6). The objective had a long working distance and a possibility of introducing a flat window (up to 2.3 mm thick) before the sample (abberation correction). This allowed putting a sample into a cryostat or a vacuum chamber.

Due to the defocusing lens, focusing of the excitation beam on the sample was not complete, and the excitation intensity profile in the sample plane had a shape close to Gaussian, perturbed with diffraction patterns (see Fig. 2 of Article I). The excitation power density in the maximum of the profile was ~150 W/cm^2.

Fluorescence light was collected with the same objective and projected onto a Photometrics Cascade 512B CCD camera chip. The camera had a high detection quantum yield, Peltier chip cooling, and a multiplication gain feature for readout noise suppression. These properties allowed achieving high signal-to-noise ra-

tios at short (fractions of a second) acquisition times. A crucial part of the setup was the system of dielectric filters and a dichroic mirror (Fig. 2.3) whose purpose was to separate the excitation and the fluorescence light. The cleanup filter ensured that only the predetermined excitation wavelength would pass through. The dichroic mirror reflected the excitation light but allowed the longer-wavelength fluorescence to pass through towards the CCD camera. The long-pass cut-off filter suppressed the remaining excitation light completely.

The setup was aligned in such a way that the objective formed an image of the sample in the plane of the slit (Fig. 2.3). The image was then projected with a lens onto the CCD. The removable holographic diffraction grating placed between the lens and the CCD served as a dispersing element. Such scheme allowed observing a sample image (as the zero order of diffraction) and spectra of the molecules (as the first order of diffraction) simultaneously (see Fig. 2.4). Note that in the case of

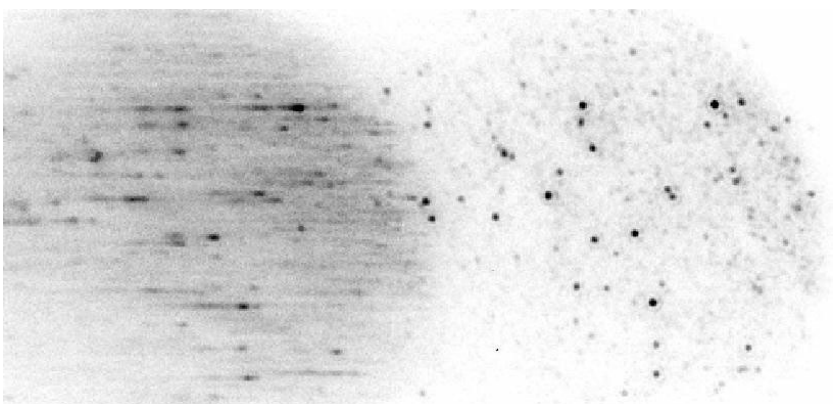

Figure 2.4: Experimental image containing both zero and first orders of diffraction (i.e. the image and spectra) of a single-molecule sample. The slit is opened completely in this case.

a single-molecule sample the size of molecule's image can serve as a spectrometer slit (as in Fig. 2.4), whereas in the case of a bulk sample the slit *has* to be used (see Fig. 2.5), and its width determines the spectral resolution.

The experimental setup has a limited fluorescence spectral range where it is operational. Besides, even within this range it is not equally sensitive at all the wavelengths. To take this into account, the setup was calibrated using a light source with a known spectrum. In this particular case, a tungsten incandescent lamp with a precise power supply was used. The resulting spectral sensitivity of the setup is shown in Fig. 2.5, top part. All the spectra presented in this work have been corrected with this sensitivity curve to allow for the non-constant spectral sensitivity of the setup.

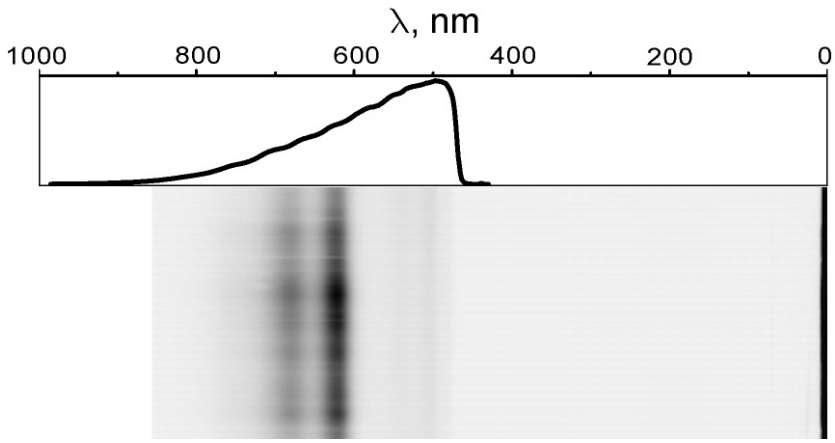

Figure 2.5: Upper part: the spectral sensitivity curve of the experimental setup. Lower part: experimental image containing both zero and first orders of diffraction (i.e. the sample image and spectra) of an MEH-PPV film at 77 K. The slit determines the spectral resolution in this case. The wavelength scale is matched for both parts of the image.

Chapter 3

From films to single molecules

3.1 Introduction

Apart from the fundamental scientific interest, one of the main incentives behind the single-molecule spectroscopy of conjugated polymers is their potential for applications. In most of the applications (such as organic light-emitting diodes or photovoltaic cells) these polymers are going to be used in the form of films. Therefore, the information we are particularly interested in is the properties of conjugated polymer films. Since single-molecule spectroscopy deals with single molecules rather than films, it is important to realize to which extent the results obtained for single molecules are relevant for films. In other words, the question is as follows: what is in common and what is the difference between an ensemble of single molecules and a bulk material?

The most obvious property of the ensemble and bulk material that should be compared to address this issue is fluorescence spectrum. This chapter contains the results of a very simple but nevertheless original study of low-temperature fluorescence spectra of MEH-PPV "films" with thicknesses ranging from tens of nanometers (bulk material) to that of discontinuous coatings with isolated molecules. An unexpectedly large dependence of fluorescence spectrum on the film thickness is demonstrated. The contents of this chapter are going to be submitted for publication.

3.2 Results and Discussion

3.2.1 Thickness-dependent MEH-PPV film spectra

A series of photoluminescence spectra of thin MEH-PPV films of different thicknesses, taken at 77 K, is shown in Fig. 3.1. All the spectra in this and subsequent

figures are recalculated to represent the number of photons per spectral interval (rather than energy). The main result here is the dramatic blue-shift ($\sim 2000\,\mathrm{cm}^{-1}$)

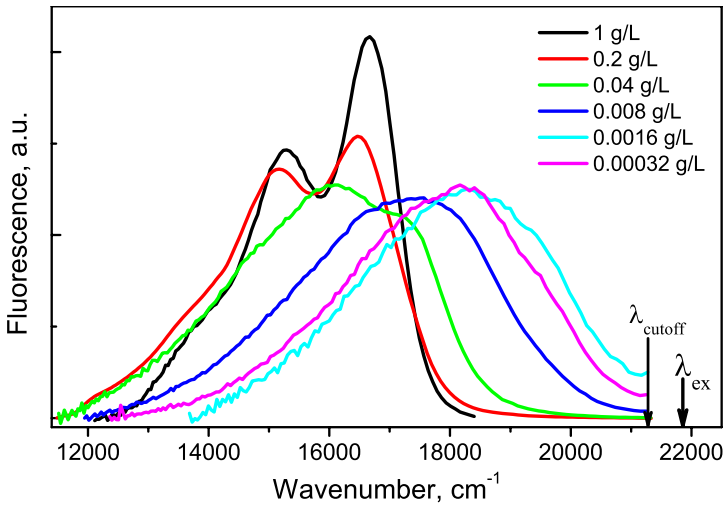

Figure 3.1: Low temperature fluorescence spectra of thin MEH-PPV films of varied thickness. T=77 K.

of the spectra with the decrease in film thickness, accompanied by a spectral broadening. In order to characterize these changes quantitatively, a sum of three Gaussian curves was fitted to the spectra. The curves represented the three spectral features in the vibronic progression (0–0, 0–1 and 0–2 transitions). The following constrains were applied during the fitting procedure:

- The three peaks are spectrally separated by a distance fixed for each graph: $E_{00} - E_{01} = E_{01} - E_{02}$. This distance equals to the vibrational energy of the C–C stretch in MEH-PPV polymer chain.

- The ratios of the peak areas satisfy the following equations: $A_{01}/A_{00} = S$, $A_{02}/A_{01} = S^2/2$, where S is the Huang-Rhys factor fixed for every graph.

To characterize the effect of film thickness variation, it is convenient to introduce an average intermolecular distance. This parameter has meaning only for sufficiently thin films where the molecules do not stack on top of each other. It can be calculated from the average surface density (number per area) of polymer monomer units and molecular weight. The surface density of monomer units can be estimated from the optical density of a film at the absorption maximum and absorption cross-section of a monomer unit at the same wavelength. Finally, the cross-section of a monomer can be calculated from optical density of a solution with a known concentration. These estimations and measurements have been

made. Absorption cross-section of an MEH-PPV monomer at the absorption maximum (≈510 nm) was found to be $\sigma_{mon} = 8.3 \cdot 10^{-17}$ cm^2. Decimal optical density of an MEH-PPV film cast from a 1 g/L solution was measured to be 0.074. This corresponds to an average surface density of monomer units n_{mon} ≈20 nm^{-2}. Assuming film density of ≈1 g/cm^3, film thickness was calculated to be 9 nm. This estimate was in a good agreement with an independent ellipsometry measurement (less than 1 nm difference). The surface density of monomers was recalculated into the surface density of molecules:

$$n_{mol} = \frac{n_{mon}}{M_N/\mu_{mon}} = 0.0275 \text{ nm}^{-2},$$

where μ_{mon} =276 g/mol is the molar mass of a monomer unit. Finally, the average intermolecular distance was obtained as follows: $d = 1/\sqrt{n_{mol}} = 6$ nm. If we assume that n_{mol} scales linearly with the solution concentration, we can obtain the values of d for all the "films".

The fitting results for E_{00} can now be presented as a function of the average intermolecular distance d (Fig. 3.2). The value of d changes from 6 nm (well-

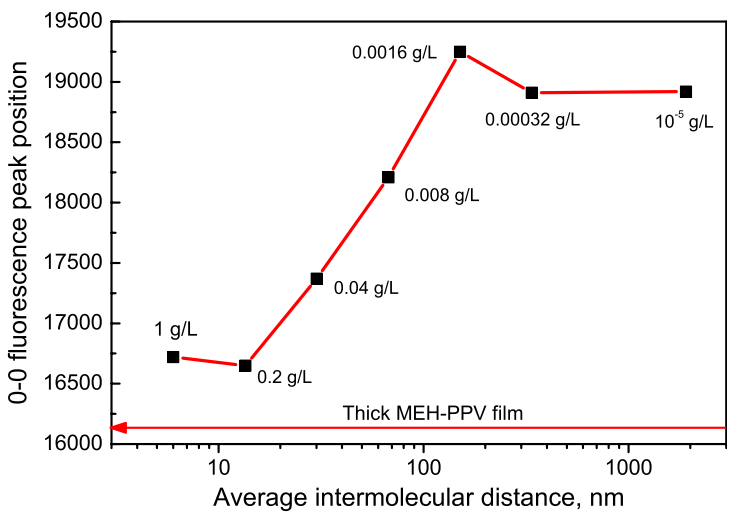

Figure 3.2: Fluorescence spectrum 0–0 peak position of thin MEH-PPV films as a function of the calculated average intermolecular distance.

overlapped molecules) for the film cast from a 1 g/L solution and goes to ≈2 μm (optically resolved molecules) for the "film" cast from a 10^{-5} g/L solution (the corresponding graph is not shown in Fig. 3.1 for clarity of the graph). As we can see from Fig. 3.2, upon the increase of d from ≈10 nm to ≈200 nm there is a transition of the 0–0 spectral peak position from ≈16600 cm^{-1} to ≈19000

cm^{-1}. Additionally, the position of 0–0 peak for a thick MEH-PPV film (obtained simply by drying a drop of 1 g/L solution on a substrate) is shown in Fig. 3.2 as a horizontal line for comparison. It is shifted to the red in comparison with the thin film spin-cast from 1 g/L solution.

3.2.2 Control experiments

One of the possible explanations of the observed dependence might be a greater photooxidation of isolated molecules due to their greater contact with remaining oxygen and SiO/SiO_2 on the substrate surface. To check whether this is the case, a control series of experiments analogous to the previous one was performed, but PMMA host matrix was used in the film preparation technique this time. MEH-PPV solution was sequentially diluted with PMMA solution so that the total polymer concentrations was kept at 2 g/L. The resulting series of spectra is shown in Fig. 3.3. As we can see, the result is similar to that of the matrix-free experiment.

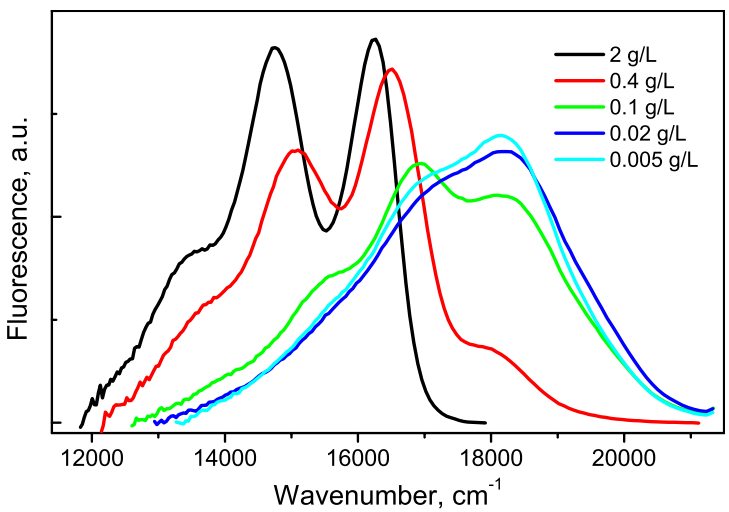

Figure 3.3: Fluorescence spectra of thin MEH-PPV/PMMA films prepared from solutions with varied MEH-PPV concentration. The total polymer concentration was 2 g/L. T=77 K.

It should be noted, however, that the spectra of MEH-PPV/PMMA composites look somewhat more structured. Additionally, to check possible influence of remaining oxygen, a series of samples was prepared in a nitrogen glove-box from a 4 g/L MEH-PPV/PMMA solution. The samples were put into a vacuum chamber inside the glove-box, then the chamber was taken out, put into the experimental setup and evacuated, preventing any contact of the films with the ambient oxy-

gen. The films exhibited the same type of structureless blue-shifted spectra at low MEH-PPV concentrations. Therefore, from the results of the control experiments it can be concluded that the effect of the spectral blue-shift is not due to chemical modification of MEH-PPV.

We are led to infer that the spectral blue-shift upon dilution of the sample is inherent to the sample structure. There may be suggested two different mechanisms by which dilution can result in the spectral blue-shift. One of them is related to excitation energy transfer, and another is related to polymer chain conformation.

3.2.3 Discussion

Conjugated polymers exhibit a large Stokes shift due to electronic relaxation in the course of energy transfer [24, 25, 23]. It means that the spectral position of fluorescence depends on excitation energy transfer. Energy transfer is affected a lot by the sample structure; in particular, the concentration of spectroscopic units affects the number of options for migration of an exciton. Therefore, in concentrated samples the excitons have more freedom to migrate to the bottom of the exciton manifold, whereas in the diluted samples the migration freedom is more limited, and the excitons end up on spectroscopic units with broader distribution (and higher average value) of excited state energy. However, the effect of the dilution should go to saturation upon reaching the concentration of isolated molecules. Isolated molecules still consist of many ($\sim$100) spectroscopic units, from which the excitons migrate to one or a few exciton traps. At the same time, in a bulk MEH-PPV film exciton migration length is $\approx$20 nm [26, 27], which corresponds to $\sim$15000 spectroscopic units (5 monomer units long each) for exciton to choose from. Hence, the difference between the energy migration effects on fluorescence spectral position in the cases of isolated molecules and a bulk film consists in choosing the trap among $\sim$100 spectroscopic units in the first case and among $\sim$15000 in the second. These two numbers have the physical meaning of the ratio of the total number of spectroscopic units to the number of exciton traps. To check how big the effect of such difference can be, a calculation was performed under the assumption of a Gaussian density of excited states (DOS). *The DOS was assumed to be the same for both cases.* It turned out to be impossible to explain the experimental result under this assumption: the difference between 15000 and 100 was not large enough to result in a 2000 cm^{-1} blue shift. Consequently, additional factors should be considered.

Another important difference that one should expect between the diluted and concentrated samples is the difference in chain packing. Tight packing of polymer chains in a bulk MEH-PPV film can result in their better alignment in comparison to that in isolated molecules [23]. Better alignment increases π-conjugation length, which, in turn, decreases excited state energy: as it follows from the exci-

ton theory, the vertical 0–0 transition energy of a spectroscopic unit as a function of the number of its monomer units is

$$E_{00}^{v}(N) = E_0 + 2\beta \cos \frac{\pi}{N+1},$$

where $E_0 = 34400$ cm^{-1} and $\beta = -8800$ cm^{-1} for MEH-PPV in chloroform [10]. Besides, tight packing can increase interaction between the chromophores substantially, because of strong distance dependence of resonance interactions ($\propto R^{-3}$) and especially dispersive interactions ($\propto R^{-6}$) [17].

In general, the effects of tight chain packing can be summarized as a change of DOS. It is clear that, by combining changes in DOS with changes in energy transfer efficiency, it is possible to explain the observed blue-shift effect. However, more research is needed to build a quantitative model describing these two mechanisms.

3.2.4 The problem of statistical representativeness

Finally, it is worth pointing out a technical difficulty inherent to single-molecule spectroscopy of π-conjugated polymers (MEH-PPV in particular). It was found (see Article I) that photoluminescence quantum yield differs a lot from one MEH-PPV molecule to the next. Because of this, a substantial part of the molecules exhibit low fluorescence intensity and, consequently, low signal-to-noise ratio. During an experiment, the choice of molecules to be investigated is done manually by an experimentalist. Quite naturally, the molecules with bad signal-to-noise ratio are disregarded. As a result, the obtained statistics is not complete. In this sense, spectral measurements of isolated-molecule "films" have an advantage over the real single-molecule spectroscopy, because they guarantee that all the molecules are included, and the result can be considered as a statistically representative ensemble spectrum of isolated molecules. Fig. 3.4 shows an example of a discrepancy arising from such a lack of representativeness in single-molecule spectroscopy. It contains an average single-molecule spectrum (which is simply a normalized sum of 27 single-molecule spectra with acceptable signal-to-noise ratio, extracted from a series of experimental images) and an ensemble spectrum of single molecules. The latter was obtained by summing up the series of images of a single-molecule sample and treating the result as an image of a bulk film (see Fig. 2.5). This approach is equivalent to taking a spectrum of an isolated-molecule "film". As one can see, there is a substantial difference between the two spectra, which implies that the choice of single molecules was not completely representative.

Also shown in Fig. 3.4 are two examples of single-molecule spectra of MEH-PPV. The spectra were chosen among the most red- and blue-shifted ones to show

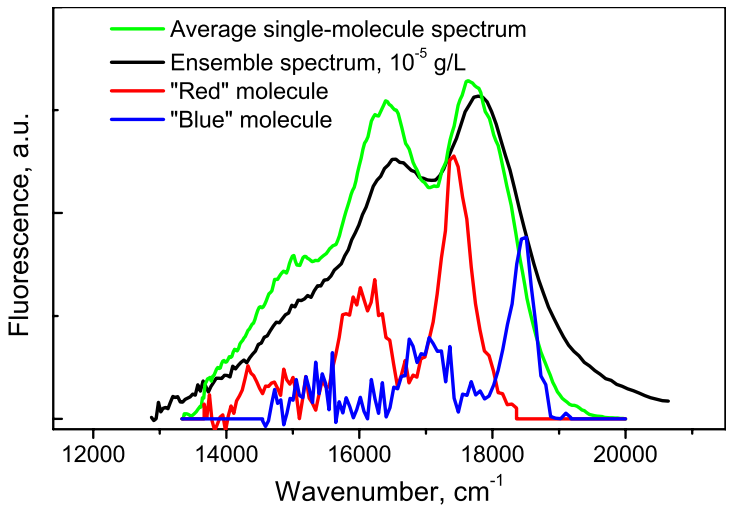

Figure 3.4: An average and ensemble fluorescence spectra of isolated MEH-PPV molecules in PMMA matrix (spin-cast from a 10^{-5}:4 g/L MEH-PPV:PMMA solution in toluene) shown together with the examples of the most red- and blue-shifted single-molecule spectra. T=77 K.

how big the difference in spectral position can be. These spectra are intrinsically the results of single-molecule spectroscopy. They contain a valuable information about the spectral properties of single polymer chains, that cannot be extracted from the experiments on isolated molecules.

3.3 Conclusions

In conclusion, two problematic aspects of single-molecule spectroscopy of π-conjugated polymers have been demonstrated. Firstly, it was shown that bulk polymer films and ensembles of single molecules possess substantially different spectral characteristics. Secondly, a problem with achieving statistical representativeness in single-molecule spectroscopy has been pointed out. These issues imply that care should be taken when generalizing single-molecule spectroscopy results to draw any conclusions about the properties of π-conjugated polymer films.

Bibliography

[1] Moerner, W. E.; Kador, L. *Phys.Rev.Lett.* **1989**, *62*(21), 2535–2538.

[2] Orrit, M.; Bernard, J. *Phys.Rev.Lett.* **1990**, *65*(21), 2716–2719.

[3] Basché, Th.; Kummer, S.; Bräuchle, C. *Nature* **1995**, *373*(6510), 132–134.

[4] Ambrose, W. P.; Moerner, W. E. *Nature* **1991**, *349*(6306), 225–227.

[5] Lu, H. P.; Xie, X. S. *Nature* **1997**, *385*(6612), 143–146.

[6] Chiang, C. K.; Fincher, C. R.; Park, Y. W.; Heeger, A. J.; Shirakawa, H.; Louis, E. J.; Gau, S. C.; MacDiarmid, A. G. *Phys.Rev.Lett.* **1977**, *39*(17), 1098–1101.

[7] Shirakawa, H.; Louis, E. J.; MacDiarmid, A. G.; Chiang, C. K.; Heeger, A. J. *J. Chem. Soc. Chem. Comm.* **1977**, (16), 578–580.

[8] Heeger, A. J. *Angew. Chem. Int. Edit.* **2001**, *40*(14), 2591–2611.

[9] Pope, M.; Swenberg, C. E. *Electronic Processes in Organic Crystals and Polymers;* Oxford University Press: New York, 2 ed., 1999.

[10] Chang, R.; Hsu, J. H.; Fann, W. S.; Liang, K. K.; Chiang, C. H.; Hayashi, M.; Yu, J.; Lin, S. H.; Chang, E. C.; Chuang, K. R.; Chen, S. A. *Chem. Phys. Lett.* **2000**, *317*(1-2), 142–152.

[11] Graham, S. C.; Bradley, D. D. C.; Friend, R. H.; Spangler, C. *Synthetic Met.* **1991**, *41*(3), 1277–1280.

[12] Brédas, J. L.; Cornil, J.; Beljonne, D.; dos Santos, D.; Shuai, Z. G. *Accounts Chem. Res.* **1999**, *32*(3), 267–276.

[13] VandenBout, D. A.; Yip, W. T.; Hu, D. H.; Fu, D. K.; Swager, T. M.; Barbara, P. F. *Science* **1997**, *277*(5329), 1074–1077.

[14] Rønne, C.; Trägårdh, J.; Hessman, D.; Sundström, V. *Chem. Phys. Lett.* **2004**, *388*(1-3), 40–45.

[15] Yu, Z. H.; Barbara, P. F. *J. Phys. Chem. B* **2004**, *108*(31), 11321–11326.

[16] Schindler, F.; Lupton, J. M.; Feldmann, J.; Scherf, U. *Proc. Nat. Acad. Sci. USA* **2004**, *101*(41), 14695–14700.

[17] Mirzov, O.; Pullerits, T.; Cichos, F.; von Borczyskowski, C.; Scheblykin, I. G. *Chem. Phys. Lett.* **2005**, *408*(4-6), 317–321.

[18] Pullerits, T.; Mirzov, O.; Scheblykin, I. G. *J. Phys. Chem. B* **2005**, *109*(41), 19099–19107.

[19] Mirzov, O.; Scheblykin, I. G. *Chem. Phys.* **2005**, *318*(3), 217–222.

[20] Yu, J.; Hu, D. H.; Barbara, P. F. *Science* **2000**, *289*(5483), 1327–1330.

[21] Mirzov, O.; Cichos, F.; von Borczyskowski, C.; Scheblykin, I. G. *Chem. Phys. Lett.* **2004**, *386*(4-6), 286–290.

[22] Mirzov, O.; Cichos, F.; von Borczyskowski, C.; Scheblykin, I. G. *J. Lumin.* **2005**, *112*(1-4), 353–356.

[23] Schwartz, B. J. *Annu. Rev. Phys. Chem.* **2003**, *54*, 141–172.

[24] Rauscher, U.; Schütz, L.; Greiner, A.; Bässler, H. *J. Phys.–Condens. Mat.* **1989**, *1*(48), 9751–9763.

[25] Kersting, R.; Lemmer, U.; Mahrt, R. F.; Leo, K.; Kurz, H.; Bässler, H.; Göbel, E. O. *Phys.Rev.Lett.* **1993**, *70*(24), 3820–3823.

[26] Savenije, T. J.; Warman, J. M.; Goossens, A. *Chem. Phys. Lett.* **1998**, *287*(1-2), 148–153.

[27] Burlakov, V. M.; Kawata, K.; Assender, H. E.; Briggs, G. A. D.; Ruseckas, A.; Samuel, I. D. W. *Phys. Rev. B* **2005**, *72*(7), 075206.

Article I

Polydispersity of the photoluminescence quantum yield in single conjugated polymer chains

O. Mirzov, I. G. Scheblykin

Reprinted from
Chemical Physics 318 (2005) 217-222

Available online at www.sciencedirect.com
SCIENCE DIRECT®
Chemical Physics 318 (2005) 217–222
Chemical Physics
www.elsevier.com/locate/chemphys

Polydispersity of the photoluminescence quantum yield in single conjugated polymer chains

O. Mirzov, I.G. Scheblykin *

Chemical Physics, Lund University, P.O. Box 124, 22100 Lund, Sweden

Received 8 April 2005; accepted 10 June 2005
Available online 14 July 2005

Abstract

The conjugated polymer poly(2-methoxy-5-(2′-ethylhexyloxy)-1,4-phenylene vinylene) (MEH-PPV) was studied by a single-molecule imaging technique. A comparison of statistical distributions of fluorescence intensity with molecular weight distributions revealed that the distribution of the photoluminescence quantum yield of the single polymer chains under study is significantly asymmetric, with a polydispersity $\gtrsim 2$. The result implies that there are molecules whose quantum yield is a few times higher than the ensemble quantum yield. This conclusion suggests a possibility of a great improvement of the photoluminescence quantum yield of MEH-PPV, which is known to be several times less than 1.

Keywords: MEH-PPV; Single-molecule spectroscopy; Photoluminescence quantum yield; Polydispersity

1. Introduction

Conjugated polymers have been attracting attention of researchers due to their great potential for various applications such as plastic solar cells, molecular electronics, and organic light-emitting diodes. One of the main characteristics of conjugated polymers, which is very important for applications, is the fluorescence quantum yield. Any information about correlation of quantum yield with other properties of conjugated polymers may be very important because it can help creating better recipes for polymer synthesis and device preparation.

During the last years, single-molecule spectroscopy and imaging proved to be powerful tools for studying a variety of systems, including conjugated polymers [1]. For conjugated polymers they have been applied to study such phenomena as fluorescence intensity fluctuations (see e.g. [2–5] and references therein) and spectral fluctuations (see e.g. [3,6,7]). To the best of our knowledge, no experimental results on the fluorescence quantum yield of single polymer chains have been reported yet [8]. Nevertheless, application of single-molecule optics to the issue of quantum yield may be especially fruitful, because it can provide information about the statistical distribution of quantum yields for single molecules (SMs), which in turn can give some insight into the nature of imperfections decreasing the quantum yield.

By definition, the photoluminescence quantum yield is the ratio of the photon emission rate to the rate of photon absorption. To determine this ratio, one can use single-molecule imaging. The photon emission rate can be calculated from the image, provided that the experimental setup has been calibrated with a reference sample. To determine the absorption rate, one needs to know the absorption cross-section and excitation intensity. The latter can be measured independently (see Section 2.1). As to the absorption cross-section, for conjugated polymer chains it can be assumed to be proportional to the

* Corresponding author. Fax: +46 46 2224119.
E-mail address: ivan.scheblykin@chemphys.lu.se (I.G. Scheblykin).
URL: http://www.chemphys.lu.se (I.G. Scheblykin).

0301-0104/$ - see front matter © 2005 Elsevier B.V. All rights reserved.
doi:10.1016/j.chemphys.2005.06.017

molecular weight, and the proportionality coefficient can be determined from the optical density of a polymer solution or film. Indeed, heavy conjugated polymer chains are known to consist of many (~100–1000) independently absorbing chromophores [9]. Besides, MEH-PPV molecules are known to coil into compact amorphous nanoparticles [4,5,10], which reduces anisotropy and polarization dependence of absorption. These facts ensure that molecule's absorption is similar to that of a bulk material (at least at room temperature).

Unfortunately, MEH-PPV samples available nowadays do not possess a well-defined molecular weight. Polymers are usually characterized by number- and weight-averaged molecular weights M_N and M_W and their ratio $P_M = M_W/M_N$ called the polydispersity index. Using a molecular weight distribution function $\rho_M(M)$ defined so that $\rho_M(M)dM$ is the fraction of the molecules having weight between M and $M + dM$, one can define M_N and M_W as follows:

$$M_N = \int M\rho_M(M)dM, \quad (1)$$

$$M_W = \frac{1}{M_N}\int M^2\rho_M(M)dM. \quad (2)$$

Some values of P_M mentioned in the literature on single-molecule studies of conjugated polymers are 2.2 [11–14], 5.7 [15], 7.6 [3], 8.0 [16]. It should be noted that no function $\rho_M(M)$, symmetric around its maximum, is likely to give $P_M \gtrsim 1.3$, and any distribution with $P_M \gtrsim 2$ is highly asymmetric, peaking at $M < M_N$ and decaying down to zero at $M > M_N$. In the latter case, M_N on its own is not informative as a characteristic of molecular weight. In this work, we used two different samples of MEH-PPV having high (7.8) and low (1.06) polydispersities. The value $P_M = 1.06$ is about the minimum that is available from MEH-PPV manufacturers, but it still corresponds to a standard deviation of ≈24% for both uniform and Gaussian weight distributions.

Hence, molecular weight is not well-defined even for the sample with $P_M = 1.06$. This makes the absorption cross-section ill-defined as well. Besides, there is another complication with measuring the quantum yield of MEH-PPV single chains: it is known that in MEH-PPV SMs excitation energy gets transferred to a few (maybe only one) chromophores [2,17]. Consequently, fluorescence is not isotropic, which may result in some distribution of the observed fluorescence intensity even for molecules having equal absorption cross-section and quantum yield and exposed to equal excitation. Thus, we cannot perform the measurement of quantum yield at once. Nevertheless, we can consider a ratio of fluorescence intensity to excitation intensity that we will in the following call "brightness" B. It is proportional to quantum yield for all molecules, provided that absorption cross-section and detection efficiency are fixed. By measuring a brightness distribution function $\rho_B(B)$ and comparing it with $\rho_M(M)$ we may be able to draw some conclusions about the quantum yield.

2. Experimental

2.1. Measurements

A wide-field fluorescence microscope was used to examine SMs of MEH-PPV with the single-molecule imaging technique. We investigated two polymer samples, purchased from American Dye Source (ADS), Inc ($M_N = 105\ 000$, $P_M \approx 7.8$) and from Aldrich (M_N is known to lie within 150 000–250 000, $P_M = 1.06$). Gel-permeation chromatography results were supplied by the manufacturer of the first sample, so it was possible to calculate $\rho_M(M)$ for it. For the second sample we may assume that it was obtained by filtering and therefore is likely to have a shape of $\rho_M(M)$ close to rectangular (knowledge of the exact shape is not important for the following). An example of what such distribution may look like (for $M_N = 200\ 000$) is shown in Fig. 1 together with the real $\rho_M(M)$ for the first sample. Note that only part of the graph is shown for the ADS sample on the linear scale.

MEH-PPV was spin-coated from toluene or chloroform solutions onto Si/SiO_2 substrates. Then a cap layer of poly(vinyl-alcohol) (PVA) was spin-coated from ~1% aqueous solution. Addition of the cap layer increased photostability of the SMs. During the experiments samples were kept in a vacuum chamber at room temperature. The 488 nm CW Ar-ion laser line was used for excitation. The beam was run through a single-mode optical fibre, which gave a Gaussian beam as output. To record the spatial excitation intensity profile in the sample plane, a fluorescence image of a uniform MEH-PPV film was taken. The profile was close to Gaussian, perturbed with diffraction patterns (Fig. 2).

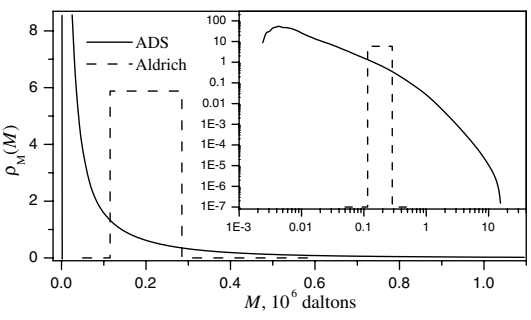

Fig. 1. The molecular weight distributions. $P_M^{(ADS)} = 7.8$, $P_M^{(Aldrich)} = 1.06$. The inset shows the same graphs on the double-logarithmic scale.

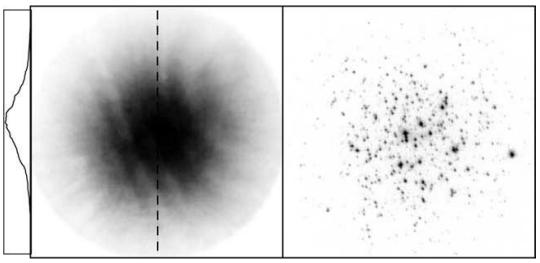

Fig. 2. The two left parts show the excitation intensity profile (measured as a fluorescence image of a uniform MEH-PPV film) and its cross-section. The right part contains an example of a single-molecule sample image.

Total excitation power was also recorded for each measurement. The average excitation power density was $\approx$50 W/cm^2. Fluorescence light was collected with an Olympus objective lens LUCPlanFI (40×, N.A. 0.6) and projected onto a Photometrics Cascade 512B CCD camera chip. Total accumulation time for each measurement was 10 s (usually 100 acquisitions, 100 ms each). In addition to the polymer samples, reference samples were investigated. These samples were prepared in absolutely the same way as the main ones, but instead of polymer solutions pure solvents were used. Images of these samples were used to estimate the contribution to resulting statistics from impurities of solvents and PVA.

2.2. Data processing

To extract brightness statistics from the obtained images, special software has been developed. The program automatically detected molecules in the images, calculated their integral signal (taking the local background level into account), and recorded excitation intensity levels at the positions of the molecules. Only molecules exposed to excitation intensity higher than 0.2 of the maximum of the excitation intensity profile were considered. The program output data were used to construct brightness distributions $\rho_B(B)$. The distributions $\rho_B(B)$ were then characterized by their polydispersity $P_B = B_B/B_N$, where B_N and B_B are defined analogously to M_N and M_W (Eqs. (1) and (2)):

$$B_N = \int B\rho_B(B)\mathrm{d}B, \tag{3}$$

$$B_B = \frac{1}{B_N}\int B^2\rho_B(B)\mathrm{d}B. \tag{4}$$

The brightness values are given here in arbitrary units, but these units are the same for all the samples, so the data can be compared. Brightness distributions of the reference samples without polymer were also calculated. To account for contribution from impurities, the reference distributions were subtracted from the main ones (before the subtraction, the distributions were renormalized to reflect number of molecules per unit area of a sample, and after the subtraction the results were normalized back to unity). This correction only altered the low-brightness tail of the distributions, resulting in no significant change of the main characteristics such as number-average and polydispersity. To check the precision of the molecule-detection program, artificial images with constant-brightness "molecules" were generated. They were prepared using a real excitation intensity profile which defined the observed intensity of the randomly positioned "molecules". An image of a reference sample without MEH-PPV was used as a background. For a test image with "molecules" having $B \approx 10$ a.u. the standard deviation of the result was $\approx$2.5% (average observed values for the real samples were within 3–8 a.u.), and for a test image with $B \approx 1$ a.u. the standard deviation was $\approx$15%. These error levels were used for Monte Carlo simulations (Section 3.2.3).

3. Results and discussion

3.1. Experimental brightness distributions

It follows from Section 1 that if all the single chains had the same photoluminescence quantum yield, the brightness distribution would reflect the distribution of the absorption cross section of the chains and hence the distribution of the molecular weight of the chains. The resulting brightness distributions obtained for the samples cast from toluene are shown in Fig. 3. The most striking result here is that the two distributions are equally broad and very similar in general. Their polydispersity indexes are 2.5 and 2.6 for ADS and Aldrich samples, respectively. Note that we cannot expect P_B to reach P_M for the ADS sample because that would require the dynamic range of the method to be $\sim 10^4$ (see the inset in Fig. 1), whereas it actually was $\sim 10^2$ (see Fig. 3). On the other hand, for the Aldrich sample $P_B = 2.6$ greatly exceeds $P_M = 1.06$. This means that

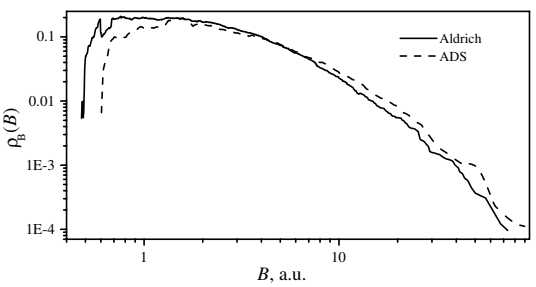

Fig. 3. Brightness distributions for the samples cast from toluene (double-logarithmic scale). $P_B^{(ADS)} = 2.5$, $P_B^{(Aldrich)} = 2.6$.

there is a broadening mechanism that breaks the proportionality between B and M. Moreover, the similarity between $\rho_B(B)$ of both samples suggests that the observed broadening is limited by the dynamic range of the method. The broadening of $\rho_B(B)$ of the Aldrich sample may arise due to the following reasons.

(1) Fluorescence intermittency, i.e. temporal fluctuations of quantum yield.
(2) Dependence of brightness on excitation intensity.
(3) Fluorescence anisotropy of SMs.
(4) Errors introduced by the data processing technique.
(5) Intrinsic variance of SM quantum yield.

Let us now consider these possible reasons in detail.

3.2. Reasons for brightness distribution broadening

3.2.1. Fluorescence intermittency

Fluorescence intermittency, or the "blinking effect", may alter the observed brightness, thereby broadening $\rho_B(B)$. Blinking has indeed been observed for MEH-PPV SMs [2]. However, at the low excitation intensity levels used in this work the effect is weak. To check it reliably, samples cast from chloroform were studied. MEH-PPV chains cast from chloroform are known to possess relatively loose conformation [10] which results in suppression of the blinking effect [3]. The brightness distributions are also very similar for both samples (not shown), although their B_N and B_B are somewhat different from those of the toluene samples (Table 1). Hence, blinking cannot explain the observed P_B.

3.2.2. Dependence of brightness on excitation intensity

Since excitation intensity differs by as much as 5 times for the considered SMs (from 0.2 to 1.0 of the maximum of the excitation intensity profile), possible dependence of brightness on excitation intensity can broaden $\rho_B(B)$. To check the presence of this effect, the Aldrich sample cast from toluene was chosen because of its largest statistics ($N_{mol} = 1870$). The molecules were split into groups having their excitation intensity within equal intervals 0.2–0.3, 0.3–0.4,...,0.9–1.0 of the maximum and a median mean [18] of brightness was calculated for each group. The results are presented in Table 2. As can be seen from the table, there is no clear dependence of $\langle B \rangle$ on W_{ex}, and the intervals containing the majority of molecules have close median means. This proves that dependence of the brightness on the excitation intensity is insignificant (if present at all) in our case.

Table 1
Experimental results comparison[a]

Solvent	Sample	B_N	B_B	P_B	N_{mol}
Toluene	ADS	8.1	20.1	2.5	260
Toluene	Aldrich	6.3	16.3	2.6	1870
Chloroform	ADS	3.3	7.6	2.3	850
Chloroform	Aldrich	4.0	7.9	2.0	780

[a] Here B_N – the number-averaged brightness, B_B – the brightness-averaged brightness, $P_B = B_B/B_N$ – the polydispersity index, and N_{mol} – the number of molecules used to construct a brightness distribution.

Table 2
Brightness as a function of excitation intensity[a]

W_{ex}	0.25	0.35	0.45	0.55	0.65	0.75	0.85	0.95
$\langle B \rangle$	3.88	3.42	3.77	3.49	3.14	2.54	4.04	3.74
N_{ex}	655	474	330	266	187	147	84	36

[a] Here W_{ex} – the middle of a corresponding excitation intensity interval, $\langle B \rangle$ – the median mean of brightness, and N_{ex} – the number of molecules falling into a corresponding interval.

3.2.3. Fluorescence anisotropy and errors

As has been mentioned above (see the end of Section 1), energy transfer to one (or a few) segments of the polymer chain results in anisotropic fluorescence, which introduces additional broadening into the observed $\rho_B(B)$. In the case of a single emitting chromophore and small numerical aperture of the microscope objective (which eliminates the angular averaging) the angular dependence of fluorescence intensity is equal to that of dipole radiation. This is the largest anisotropy we may expect. To consider this effect together with the data processing errors (see Section 2.2), a Monte Carlo simulation of $\rho_B(B)$ was performed with the Mathcad calculation software, using the following assumptions.

- The fluorescence quantum yield is constant.
- The molecule's absorbance is proportional to its mass, but emission comes from a single dipole with random arbitrary orientation. Objective has N.A. $\ll 1$.
- $\rho_M(M)$ equals to that of the Aldrich sample shown in Fig. 1, $P_M = 1.06$.
- The resulting distribution is broadened in order to simulate the errors of the technique.

The program generated a series of "molecules" with random weight M (distributed accordingly to the assumed $\rho_M(M)$) and random orientations of their emitting dipoles. The orientations were uniformly distributed over the whole solid angle of 4π. The observed brightness of a molecule was then taken to be $\sim M \sin^2\theta$, where θ is the angle between the emitting dipole orientation and the direction from the molecule to the detector. The proportionality coefficient was the same for all the molecules, and its value was chosen so as to obtain B_N equal to that of a corresponding experimental distribution. Finally, some noise was added to the obtained brightness values to simulate the experimental errors (see Section 2.2).

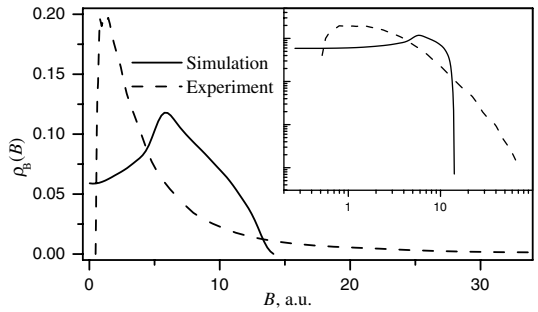

Fig. 4. The simulated brightness distribution in comparison with the experimental result. $P_B^{(simul)} = 1.3$, $P_B^{(exper)} = 2.6$. The inset shows the same graphs on the double-logarithmic scale.

The simulated brightness distribution is shown in Fig. 4 together with the experimental result for the Aldrich sample cast from toluene. The resulting distribution has a polydispersity index $P_B = 1.3$. It should be noted that the value $P_B = 1.3$ is an upper estimate, since the largest possible fluorescence anisotropy was assumed. Yet even this value is much smaller than $P_B = 2.6$ of the experimental distribution. This means that apart from intrinsic variance of quantum yield, all the possible reasons for the observed broadening of $\rho_B(B)$ have been rejected.

3.3. Polydispersity of the quantum yield distribution

Thus, we conclude that the distribution of quantum yield of single MEH-PPV chains under study $\rho_Q(Q)$ has a significant width. Moreover, from the large difference between the model and experimental polydispersities it is apparent that $\rho_Q(Q)$ itself has a large polydispersity P_Q. To estimate P_Q, the above simulation was extended to replace the constant quantum yield with the quantum yield distribution, which was assumed to be independent from molecular weight. To simulate the quantum yield distribution, the quantum yield was represented as a random value $\sim [\mathcal{N}(1, 0.2)]^{\alpha}$, where $\mathcal{N}(1, 0.2)$ is a normally distributed random value with a unit mean and a standard deviation of 0.2, and α is a tunable parameter. The choice of random value was mainly determined by technical convenience. The parameter α was tuned so as to give the model P_B equal to that of the experimental brightness distribution. The resulting value of α was 5.2 and the corresponding model distribution $\rho_Q(Q)$ is shown in Fig. 5. Note that it should be considered as a qualitative illustration rather than a quantitative result. The distribution is presented in relative units, because the relative quantum yield $Q_{rel} = Q/Q_N$ is addressed here instead of the absolute quantum yield Q (here Q_N is the number-averaged quantum yield). It does not affect the polydispersity, which is equal to 2.1 for the model distribution. It should be noted again, that this is a lower estimate since the largest possible P_B was taken for the case of fixed Q.

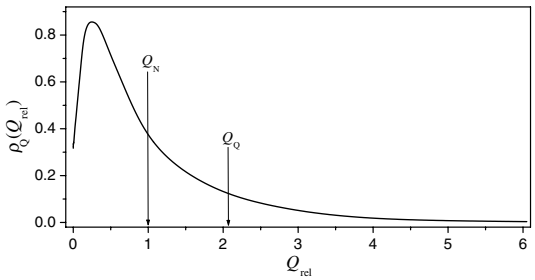

Fig. 5. The estimated model distribution of relative quantum yield $Q_{rel} = Q/Q_N$. $P_Q = 2.1$.

As can be seen from Fig. 5, $\rho_Q(Q)$ is asymmetric with a maximum below the average value (which is equal to unity by definition of Q_{rel}) and a long tail extending well above it. Hence, most of the molecules in our samples have low quantum yield compared to a possible maximum, and only a very small part of them approach this "defect-free" limit. It is interesting to note that the number-averaged quantum yield Q_N has the physical meaning of ensemble quantum yield – the quantity measured by non-single-molecule techniques. So, one may summarize the results of this work as follows: the ensemble quantum yield of the MEH-PPV molecules under study is a few times smaller than the potentially achievable value. This means that the sample-preparation technique (including polymer synthesis, sample structure and preparation recipe) must have a dramatic influence on the fluorescence quantum yield. To check the possible significance of the sample structure, a control experiment was performed on samples, where MEH-PPV was mixed with a polymer matrix (as in e.g. [2,6]). It resulted in similar brightness distributions, which implies that it is the polymer itself rather than the sample structure that determine the high value of P_Q. The studies of photoluminescence quantum efficiency for an MEH-PPV film give the result 10–15% [19]. In the light of the above discussion, these values suggest that there is a room for a great improvement of the quantum yield.

3.4. Conclusions

In conclusion, we have demonstrated a technique for indirect characterization of fluorescence quantum yield distributions of single conjugated polymer molecules. Application to MEH-PPV showed that the quantum yield distribution is very asymmetric with polydispersity $\gtrsim 2$, implying the presence of numerous defects lowering the quantum yield of the most of the molecules. The technique can be developed further, allowing estimation of absolute quantum yield.

Acknowledgements

This work was supported by Swedish Research Council, Knut&Alice Wallenberg foundation, and Crafoord foundation. O.M. is grateful to the Swedish Institute and Kungl. Fysiografiska Sällskapet. The authors also thank Villy Sundström and Tõnu Pullerits for valuable discussions and Ralph Hania for technical help.

References

[1] F. Kulzer, M. Orrit, Annu. Rev. Phys. Chem. 55 (2004) 585.
[2] D.A. VandenBout, W.T. Yip, D.H. Hu, D.K. Fu, T.M. Swager, P.F. Barbara, Science 277 (1997) 1074.
[3] T. Huser, M. Yan, L.J. Rothberg, Proc. Nat. Acad. Sci. USA 97 (2000) 11187.
[4] O. Mirzov, F. Cichos, C. von Borczyskowski, I.G. Scheblykin, Chem. Phys. Lett. 386 (2004) 286.
[5] O. Mirzov, F. Cichos, C. von Borczyskowski, I.G. Scheblykin, J. Lumin. 112 (2005) 353.
[6] F. Schindler, J.M. Lupton, J. Feldmann, U. Scherf, Proc. Nat. Acad. Sci. USA 101 (2004) 14695.
[7] O. Mirzov, T. Pullerits, F. Cichos, C. von Borczyskowski, I.G. Scheblykin, Chem. Phys. Lett. 408 (2005) 317.
[8] G.M. Svishchev, Opt. Spectrosc+. 97 (2004) 340.
[9] M. Pope, C.E. Swenberg, Electronic Processes in Organic Crystals and Polymers, second ed., Oxford University Press, New York, 1999.
[10] B.J. Schwartz, Annu. Rev. Phys. Chem. 54 (2003) 141.
[11] D.H. Hu, J. Yu, P.F. Barbara, J. Am. Chem. Soc. 121 (1999) 6936.
[12] Z.H. Yu, P.F. Barbara, J. Phys. Chem. B 108 (2004) 11321.
[13] J.D. White, J.H. Hsu, S.C. Yang, W.S. Fann, G.Y. Pern, S.A. Chen, J. Chem. Phys. 114 (2001) 3848.
[14] C.F. Wang, J.D. White, T.L. Lim, J.H. Hsu, S.C. Yang, W.S. Fann, K.Y. Peng, S.A. Chen, Phys. Rev. B 67 (2003) 035202.
[15] S.S. Sartori, S. De Feyter, J. Hofkens, M. Van der Auweraer, F. De Schryver, K. Brunner, J.W. Hofstraat, Macromolecules 36 (2003) 500.
[16] P. Kumar, A. Mehta, M.D. Dadmun, J. Zheng, L. Peyser, A.P. Bartko, R.M. Dickson, T. Thundat, B.G. Sumpter, D.W. Noid, M.D. Barnes, J. Phys. Chem. B 107 (2003) 6252.
[17] J. Yu, D.H. Hu, P.F. Barbara, Science 289 (2000) 1327.
[18] W.H. Press, S.A. Teukolsky, W.T. Vetterling, B.P. Flannery, Numerical Recipes in C – The Art of Scientific Computing, second ed., Cambridge University Press, Cambridge, MA, 1992.
[19] N.C. Greenham, I.D.W. Samuel, G.R. Hayes, R.T. Phillips, Y.A.R.R. Kessener, S.C. Moratti, A.B. Holmes, R.H. Friend, Chem. Phys. Lett. 241 (1995) 89.

Acknowledgements

First of all, I would like to acknowledge the help, collaboration and support of my supervisors, Dr. Ivan Scheblykin and Prof. Villy Sundström. Thank you for accepting me into the Department and providing me with everything that is needed for a good start and progress of PhD studies.

Also, I'd like to thank our senior colleagues Drs. Tõnu Pullerits and Arkady Yartsev, as well as our closest collaborator Dr. Ralph Hania and others for the stimulating discussions we have had.

I'm grateful to Heleen Hjalmarsson, the secretary of our Department, for helping me with many practical things.

A big thanks goes to Dr. Han-Kwang Nienhuys for introducing me to LaTeX.

Generally, I would like to thank all the members of the Department of Chemical Physics for the friendly and creative atmosphere you are maintaining. Also, thank you for all the Fikas, Coffee breaks, Christmas parties, Spring trips, Departmental lunches, etc.